Brain Imaging and Behavior (2012) 6:329–342
DOI 10.1007/s11682-012-9175-2

mTBI SPECIAL ISSUE

Robust detection of traumatic axonal injury in individual mild traumatic brain injury patients: Intersubject variation, change over time and bidirectional changes in anisotropy

Michael L. Lipton · Namhee Kim · Young K. Park · Miriam B. Hulkower · Tova M. Gardin · Keivan Shifteh · Mimi Kim · Molly E. Zimmerman · Richard B. Lipton · Craig A. Branch

Published online: 9 June 2012

Abstract To identify and characterize otherwise occult inter-individual spatial variation of white matter abnormalities across mild traumatic brain injury (mTBI) patients. After informed consent and in compliance with Health Insurance Portability and Accountability Act (HIPAA), Diffusion tensor imaging (DTI) was performed on a 3.0 T MR scanner in 34 mTBI patients (19 women; 19–64 years old) and 30 healthy control subjects. The patients were imaged within 2 weeks of injury, 3 months after injury, and 6 months after injury. Fractional anisotropy (FA) images were analyzed in each patient. To examine white matter diffusion abnormalities across the entire brain of individual patients, we applied Enhanced Z-score Microstructural Assessment for Pathology (EZ-MAP), a voxelwise analysis optimized for

M. L. Lipton (✉) · N. Kim · Y. K. Park · M. B. Hulkower · T. M. Gardin · C. A. Branch
The Gruss Magnetic Resonance Research Center,
Albert Einstein College of Medicine of Yeshiva University,
1300 Morris Park Avenue,
Bronx, NY 10461, USA
e-mail: michael.lipton@einstein.yu.edu

M. L. Lipton · N. Kim · C. A. Branch
Department of Radiology,
Albert Einstein College of Medicine of Yeshiva University,
1300 Morris Park Avenue,
Bronx, NY 10461, USA

M. L. Lipton
Department of Psychiatry & Behavioral Sciences,
Albert Einstein College of Medicine of Yeshiva University,
1300 Morris Park Avenue,
Bronx, NY 10461, USA

M. L. Lipton
The Dominick P Purpura Department of Neuroscience,
Albert Einstein College of Medicine of Yeshiva University,
1300 Morris Park Avenue,
Bronx, NY 10461, USA

M. Kim · R. B. Lipton
Department of Epidemiology and Population Health,
Albert Einstein College of Medicine of Yeshiva University,
1300 Morris Park Avenue,
Bronx, NY 10461, USA

M. E. Zimmerman · R. B. Lipton
The Saul R. Korey Department of Neurology,
Albert Einstein College of Medicine of Yeshiva University,
1300 Morris Park Avenue,
Bronx, NY 10461, USA

C. A. Branch
Department of Physiology & Biophysics,
Albert Einstein College of Medicine of Yeshiva University,
1300 Morris Park Avenue,
Bronx, NY 10461, USA

M. L. Lipton · T. M. Gardin · K. Shifteh
The Department of Radiology, Montefiore Medical Center,
111 East 210th Street,
Bronx, NY 10467, USA

Present Address:
Y. K. Park
Hofstra North Shore-LIJ School of Medicine at Hofstra University,
North Shore-Long Island Jewish Health System,
300 Community Drive,
Manhasset, NY 11030, USA

the assessment of individual subjects. Our analysis revealed areas of abnormally low or high FA (voxel-wise P-value< 0.05, cluster-wise P-value<0.01(corrected for multiple comparisons)). The spatial pattern of white matter FA abnormalities varied among patients. Areas of low FA were consistent with known patterns of traumatic axonal injury. Areas of high FA were most frequently detected in the deep and subcortical white matter of the frontal, parietal, and temporal lobes, and in the anterior portions of the corpus callosum. The number of both abnormally low and high FA voxels changed during follow up. Individual subject assessments reveal unique spatial patterns of white matter abnormalities in each patient, attributable to inter-individual differences in anatomy, vulnerability to injury and mechanism of injury. Implications of high FA remain unclear, but may evidence a compensatory mechanism or plasticity in response to injury, rather than a direct manifestation of brain injury.

Keywords Mild traumatic brain injury (mTBI) · MRI · Diffusion tensor imaging (DTI) · Traumatic axonal injury (TAI) · Image processing and analysis

Abbreviations

CT	Computerized tomography
DTI	Diffusion tensor imaging
EZ	Enhanced Z-score
EZ-MAP	Enhanced Z-score microstructural assessment for pathology
FA	Fractional anisotropy
GCS	Glasgow Coma Scale
GRF	Gaussian Random Field
HIPAA	Health Insurance Portability and Accountability Act
IRB	Institutional Review Board
JHU	Johns Hopkins University
MNI	Montreal Neurological Institute
MR	Magnetic resonance
mTBI	Mild traumatic brain injury
ROC	Receiver operating characteristic
SD	Standard deviation
TAI	Traumatic axonal injury
TBI	Traumatic brain injury

Introduction

Diagnosis of mild traumatic brain injury (mTBI) is typically based on history and examination. Diagnostic criteria include Glasgow Coma Scale (GCS) of 13–15, loss of consciousness not exceeding 20 min, posttraumatic amnesia not exceeding 24 h and absence of neurological deficits (Esselman and Uomoto 1995) (see Messé, et al. in this issue). Animal studies (Povlishock 1992; Crooks 1991; Pettus et al. 1994; Povlishock 1986; Povlishock et al. 1983; Rubovitch et al. 2011; Greer et al. 2011; Spain et al. 2010) indicate that TBI, including mild injury (Povlishock et al. 1983; Rubovitch et al. 2011; Greer et al. 2011; Spain et al. 2010), results in traumatic axonal injury (TAI), the presumptive pathological substrate of clinical deficits seen in humans (Meythaler et al. 2001; Sharp and Ham 2011; Little et al. 2010) (see Bigler and Maxwell 2012). Despite the strong consensus that clinical manifestations of mTBI are a consequence of TAI, widely used diagnostic tests such as CT and MR imaging, generally have not provided evidence of brain abnormalities (Hammoud and Wasserman 2002).

Diffusion tensor imaging (DTI) reveals evidence of TAI in animal models of TBI (e.g., (Mac Donald et al. 2007a, b; Wang et al. 2009)) and in patients, where brain abnormalities detected by DTI are associated with important clinical outcomes (e.g.,(Kraus et al. 2007; Miles et al. 2008; Niogi et al. 2008a)). Recent studies have used DTI to link specific functional impairment after mTBI to injury at specific brain regions (e.g.,(Niogi et al. 2008b; Geary et al. 2010; Little et al. 2010; Levin et al. 2010; Hartikainen et al. 2010; Lipton et al. 2009)). (See Shenton, et al. 2012) These studies compare groups of patients, implicitly assuming that location of injury will be the same across patients. However, the wide variation in the direction and magnitude of forces applied during head injury makes this assumption highly improbable (Kou et al. 2010; Muller et al. 2009) (see Rosenbaum and Lipton 2012). In addition, DTI must be analyzed at the individual subject level to be useful as a patient-oriented diagnostic tool.

We have developed a whole brain assessment of Fractional Anisotropy (FA) optimized for assessment of individual patients, which we have termed "Enhanced Z-score Microstructural Analysis for Pathology" (EZ-MAP), showing that it discriminates mTBI patients from controls at the time of injury (Kim et al. 2011). Herein we apply this method to the assessment of a cohort of mTBI patients at multiple times after injury to directly assess the utility of the approach and the inter-subject variation in TAI pathology that it reveals.

Materials and methods

Study subjects

After Institutional Review Board (IRB) approval, compliance with the Health Insurance Portability and Accountability Act (HIPAA) and written informed consent, subjects were prospectively enrolled, distinct from clinical care.

mTBI patients Thirty-four consecutive patients with mTBI, meeting inclusion and exclusion criteria (Table 1), were recruited from the emergency department of a single urban hospital between August 2006 and May 2010. Patients

Table 1 Inclusion and exclusion criteria

	Inclusion criteria	Exclusion criteria
Patients	1. 18–67 years of age	1. Prior head injury
	2. Emergency department diagnosis of concussion within 2 weeks	2. Hospitalization due to the injury
	3. GCS=13–15	3. Neurodevelopmental or neurological disorder
	4. LOC<20 min	4. Major psychiatric disorder
	5. Posttraumatic amnesia <24 h	5. Illicit drug use within 30 days
	6. No focal neurologic deficit	6. Skull fracture or abnormal CT
	7. English or Spanish proficiency	
Normal subjects	1. 18–67 years of age	Same as for patients

presented 2–14 days following mild head injury due to falls (n=16), assault (n=11), motor vehicle accidents (n=5), impact by a moving object (n=3) or sports (n=1). Follow-up imaging was performed at 3 months (n=16) and 6 months (n=10) after injury.

Control subjects Thirty control subjects, with age and gender distribution encompassing that of the patients, were recruited through advertisements. Control subjects underwent the same MR imaging protocol as patients. Similarity of the patient and control groups was confirmed with χ^2 (gender) and Student t (age) tests. Controls met the same exclusion criteria applied to patients, including (a) history of prior head injury, (b) history of neurologic or psychiatric disease, and (c) history of illicit drug use.

Data acquisition

Imaging was performed using a 3.0 T MRI scanner (Achieva; Philips Medical Systems, Best, the Netherlands) with an eight-channel head coil (Sense Head Coil; Philips Medical Systems). T1-weighted whole-head structural imaging was performed using sagittal three-dimensional magnetization-prepared rapid acquisition gradient echo (MP-RAGE; TR/TE=9.9/4.6 msec; field of view, 240 mm^2; matrix, 240×240; and section thickness, 1 mm). T2-weighted whole-head imaging was performed using axial two-dimensional turbo spin-echo (TR/TE=4000/100 msec; field of view, 240 mm^2; matrix, 384×512; and section thickness, 4.5 mm) and axial two-dimensional fluid-attenuated inversion recovery turbo spin-echo (TR/TE=1100/120 msec; inversion time, 2800 msec; field of view, 240 mm^2; matrix, 384×512; section thickness, 4.5 mm; and number of signals acquired, one) imaging. DTI was performed using single-shot echo-planar imaging (TR/TE=3800/88 msec; field of view, 240 mm^2; matrix, 112×89; section thickness, 4.5 mm; independent diffusion sensitizing directions, 32; and b=1000 s/mm^2).

Data analysis

Data quality control Phantom and actual experimental data are checked for signal-to-noise, geometric distortion and other artifacts as well as head motion during the DTI acquisition. Data of poor quality or with significant gross motion are excluded from analysis.

Neuroradiologic image assessment Two American Board of Radiology certified neuroradiologists independently reviewed MR images of all subjects (patients and controls) in random sequence during a single session, blind to clinical information and group membership (patient or control).

Calculation of diffusion parameter images The 33 diffusion-weighted image sets (32 diffusion sensitizing directions and the b=0 s/mm^2 image) were corrected for head motion and eddy current effects using an affine registration algorithm. FA was derived from DTI at each voxel using the FMRIB Diffusion Toolbox (Smith et al. 2007).

Image analysis Quantitative image analysis was performed as follows:

Skull stripping:

Non-brain voxels were removed from the MP-RAGE and turbo spin-echo images using FMRIB-FSL software (Smith et al. 2004). Each brain volume was inspected section-by-section, and residual non-brain voxels were removed manually.

Echo-planar imaging distortion correction:

Turbo spin-echo images were acquired with the same section thickness, position and orientation as DTI. Distortion correction was accomplished using a nonlinear deformation algorithm to match each echo-planar image to the corresponding co-planar turbo spin-echo image (Lim et al. 2006).

Intermediate rigid-body registration:

Each subject's turbo spin-echo images were registered to their three-dimensional MP-RAGE volume using the Automated Registration Toolbox three-dimensional rigid-body approach (Ardekani 1995; Ardekani et al. 2005).

Registration to standard space:

The nonlinear registration module of the Automated Registration Toolbox was used to register each subject's three-dimensional MP-RAGE volume to a standard T1-weighted template (Montreal Neurological Institute atlas; MNI) (Holmes et al. 1998).

Transformation of DTI to standard space:

Using the Automated Registration Toolbox, distortion correction, intermediate rigid-body registration, and standard space registration were applied to the calculated FA maps in a single resectioning operation. Final cubic voxel size was 1 mm^3, masked to exclude non-brain voxels from the analysis.

Registration assessment:

Our spatial normalization procedure has been shown to be robust across subjects (Ardekani 1995; Ardekani et al. 2005). Nonetheless, the results of each registration are critically assessed by viewing each stage of the registration output, with particular assessment of the alignment of (1) brain surface, (2) deep structures including brainstem, corpus callosum and fornix and (3) grey/white margin in both the deep grey structures and at the cortical margin. These landmarks must align within one-two voxel dimensions for the registration to be accepted, although alignment is typically nearly exact.

White matter segmentation:

The fast automated segmentation tool in the FMRIB-FSL package (Smith et al. 2004) was used to generate a white matter mask for the three-dimensional MP-RAGE template brain images. This mask was eroded by 3 voxels, to eliminate locations most at risk of misregistration, and was used to restrict subsequent statistical analysis of FA to white matter voxels.

Subregion segmentation:

The Johns Hopkins University (JHU) white matter atlas (Oishi et al. 2010) was adapted for segmentation of white matter subregions. Using FLIRT from the FMRIB-FSL package (Smith et al. 2004), the T1-weighted JHU white matter atlas was registered to the T1-weighted template. The resulting transformation matrix was applied to the white matter segmentation volume of the JHU white matter atlas to bring it into registration with the MNI template used for DTI analysis.

Prior to subsequent voxelwise analyses, multiple linear regression analysis of the effects of age, gender, and education was performed within 30 control subjects. Regression coefficients were applied to the voxels within each patient's FA image where effects of covariates on individual control FA voxels were significant at $p<0.05$ and more than 100 significant voxels formed a contiguous cluster.

Enhanced Z-score (EZ) analysis:

Details of the analysis procedure are provided in the Appendix. Briefly, the whole-brain voxel-wise Z-score, optimized for assessment of individual patients, was used to identify loci with abnormally low or abnormally high FA in each individual patient compared to the control group. This technique has been optimized and validated previously (Kim et al. 2011). The analysis was performed separately for each patient's spatially normalized (Montreal Neurological Institute (MNI)) brain volume and includes the following steps: (1) The FA volume for each patient is adjusted for demographic covariates (above). (2) Robust estimation of the control population variance is achieved using a bootstrap resampling procedure. (3) The Enhanced Z-score is computed independently for each voxel in a given patient's FA volume, using the variance determined from step 1. (4) The Enhanced Z-score map thus generated is thresholded to exclude voxels that do not meet criteria for significant deviation from the control distribution. We accept as significant deviations only clusters of voxels which meet two criteria: (a) $|EZ|>1.96$ for each voxel and (b) $p<0.01$ for the cluster size among voxels meeting the initial EZ-score criterion (a); the cluster size threshold is corrected for multiple comparisons.

Results

The patient and control populations did not differ significantly with respect to age or gender (Table 2). There was a difference in education ($P=0.0002$) between controls and patients, but this was adjusted for by applying regression parameters to the FA images, as described above. Structural MRI (i.e., images other than DTI) did not show evidence of hemorrhage, edema, structural or signal abnormalities, or other gross evidence of TBI.

Areas of abnormally low FA were detected in 32 of 34 patients within 2 weeks of injury, in areas typically associated with traumatic axonal injury including the corona radiata (anterior and superior), splenium of the corpus callosum, precentral white matter, internal capsule, and deep and subcortical white matter (Table 3). Areas of abnormally high FA were detected in 32 of 34 patients, most frequently in the corona radiata (anterior and superior), deep and subcortical frontal white matter, and in the genu and body of the corpus callosum. Abnormally high FA was found in the splenium of the corpus callosum of only 6 out of 34 subjects (Table 4). The spatial pattern of white matter FA abnormalities varied from patient to patient (Fig. 1). To facilitate comparison among subjects and timepoints, we have generally displayed results overlaid on the template brain. However, display of results for a given subject on their own structural brain volume (Fig. 2) may also be useful, particularly in assessing DTI abnormalities in relation to other structural abnormalities, if they are present.

Most patients who were imaged at 3 months post-injury (Fig. 3) were found to have areas of abnormally high (15/16) and low (14/16) FA. Eleven of these 16 patients had a greater number of abnormally high FA voxels when compared to their initial measurement (Table 5). Ten of the 16

Table 2 Subject characteristics

Patient data	Patients (n=34)	Controls (n=30)	P Value
Age (y)			
Men	29.9±6.4	36.6±11.9	0.07
Women	38.9±13.2	38.1±10.3	0.81
Total	34.9±11.5 (19–64)	37.3±11.0 (20–60)	0.44
No. of men**	44 %(15/34)	53 % (16/30)	0.11
Education (y)	13.1±2.9 (8–19)	17.0±4.4 (7–26)	0.0002

Note- mean ± standard deviation (range), unless otherwise indicated

**Number of patients (percentages)

patients had fewer abnormally low FA voxels when compared to their initial assessments (Table 5). We found an overall trend toward greater number of abnormally high FA voxels and lesser number of abnormally low FA voxels at 3 months, in comparison to the initial assessment (within 2 weeks of mTBI).

Ten patients returned for follow-up at 6 months post-injury (Fig. 4). Abnormally high FA voxels were detected in all patients completing this follow-up evaluation whereas abnormally low FA voxels were detected in only 7 patients. Six out of 10 patients had fewer abnormally high FA voxels when compared to either of their earlier assessments. Five out of 10 patients had fewer abnormally low FA voxels when compared to either of their earlier assessments. Overall, the trend of temporal change differed between abnormally low and high FA. We found the most abnormally high FA voxels at 3 months, with a subsequent decrease at 6 months. The number of abnormally low FA voxels, however, declined at 3 months and still further at 6 months (Table 6).

To determine areas where similar brain loci were abnormal across patients, we performed a 1-sample T-test on the EZ maps from each of the 7 patients who completed all 3 assessments. The null hypothesis was that the mean EZ of patients at a given location would be equal to zero. Thus, a determination to reject the null hypothesis would indicate a significant deviation from the control group mean at that location. Details of the 1-sample T-test are provided in the Appendix. Results are shown in Fig. 5, demonstrating increasing number of abnormally high FA voxels at 3 months followed by a decrease at 6 months. The number of abnormally low FA voxels decreases steadily at 3 and 6 months. These results allow us to quantify the change in the extent of abnormally low or high FA regions over time and support the patterns we found in individual patients (See Figs. 1, 3, 4).

We also employed an alternate approach to quantify change over time. A voxelwise paired t-test was performed across the same group of subjects, separately comparing the first vs. second and the second vs. third follow-up assessments. These results (Fig. 6) quantify the extent and direction of change over time, not change in the prevalence of abnormal FA voxels (as in the 1-sample t-test) and therefore depict a somewhat different spatial pattern than seen in Fig. 5.

Discussion

We employed EZ-MAP to reveal evidence of TAI in individual mTBI patients at a range of times following injury. We thus add to the body of evidence indicating that brain tissue injury occurs after mild head trauma, even when conventional MR images appear normal (see Bigler and Maxwell 2012). Our study breaks important new ground,

Table 3 Frequently observed regions with abnormally low FA within 2 weeks of mTBI

Regions	Number of patients out of 34	%
Superior corona radiata (R)	15	44.1(=15/34)
Anterior corona radiata (R)	14	41.2(=14/34)
Splenium of corpus callosum (L)	14	41.2(=14/34)
Superior corona radiata (L)	14	41.2(=14/34)
Precentral WM (R)	12	35.3(=12/34)
Posterior Limb of internal capsule (R)	12	35.3(=12/34)
Posterior thalamic radiation (L)	12	35.3(=12/34)
Middle occipital WM (R)	11	32.4(=11/34)
Splenium of corpus callosum (R)	11	32.4(=11/34)
Body of corpus callosum (R)	11	32.4(=11/34)
Posterior limb of internal capsule (L)	11	32.4(=11/34)
Precentral WM (L)	10	29.4(=10/34)
Retrolenticular internal capsule (L)	10	29.4(=10/34)

Patients were only considered to have an abnormality within a region if at least 100 significantly abnormal voxels were present in that region

Table 4 Frequently observed regions with abnormally high FA within 2 weeks of mTBI

Regions	Number of patients out of 34	%
Anterior corona radiata (R)	21	61.8(=21/34)
Superior corona radiata (R)	19	55.9(=19/34)
Body of corpus callosum (R)	17	50.0(17/34)
Superior corona radiata (L)	17	50.0(=17/34)
Anterior corona radiata (L)	17	50.0(=17/34)
Genu of corpus callosum (R)	15	44.1(=15/34)
Body of corpus callosum (L)	13	38.2(=13/34)
Superior frontal WM (R)	12	35.3(=12/34)
Posterior corona radiata (L)	11	32.4(=11/34)
Putamen (R)	10	29.4(=10/34)
Posterior corona radiata (R)	10	29.4(=10/34)
Putamen (L)	10	29.4(=10/34)

Patients were only considered to have an abnormality within a region if at least 100 significantly abnormal voxels were present in that region

however, by demonstrating significant inter-individual differences in TAI. Although several brain regions are consistently affected across most patients, the pattern of abnormalities is unique in each individual. This finding may be explained by the interaction of the unique characteristics of each patient and the particular biomechanical features of each injury. The fact that certain brain areas (e.g., corpus callosum) are commonly abnormal likely reflects a greater susceptibility of these structures to TBI, as described in prior studies of diffuse axonal injury (e.g., McArthur et al. 2004). Even within these susceptible structures, however, the pattern, extent and magnitude of the abnormalities are variable. Variation of mTBI pathology between patients should be expected. Consideration of inter-individual variation may improve diagnosis and prognosis based on DTI and provide a useful individualized proxy endpoint for future clinical trials of TBI treatment. We emphasize that the intersubject variation seen here would be left undetected in a group-wise analysis. See Rosenbaum and Lipton 2012, which discusses the issue of intersubject variation in mTBI.

We chose to study FA because it has been the diffusion parameter most widely explored and has yielded the greatest number of findings in TBI. Several studies have supported the use of FA for identifying white matter abnormalities in

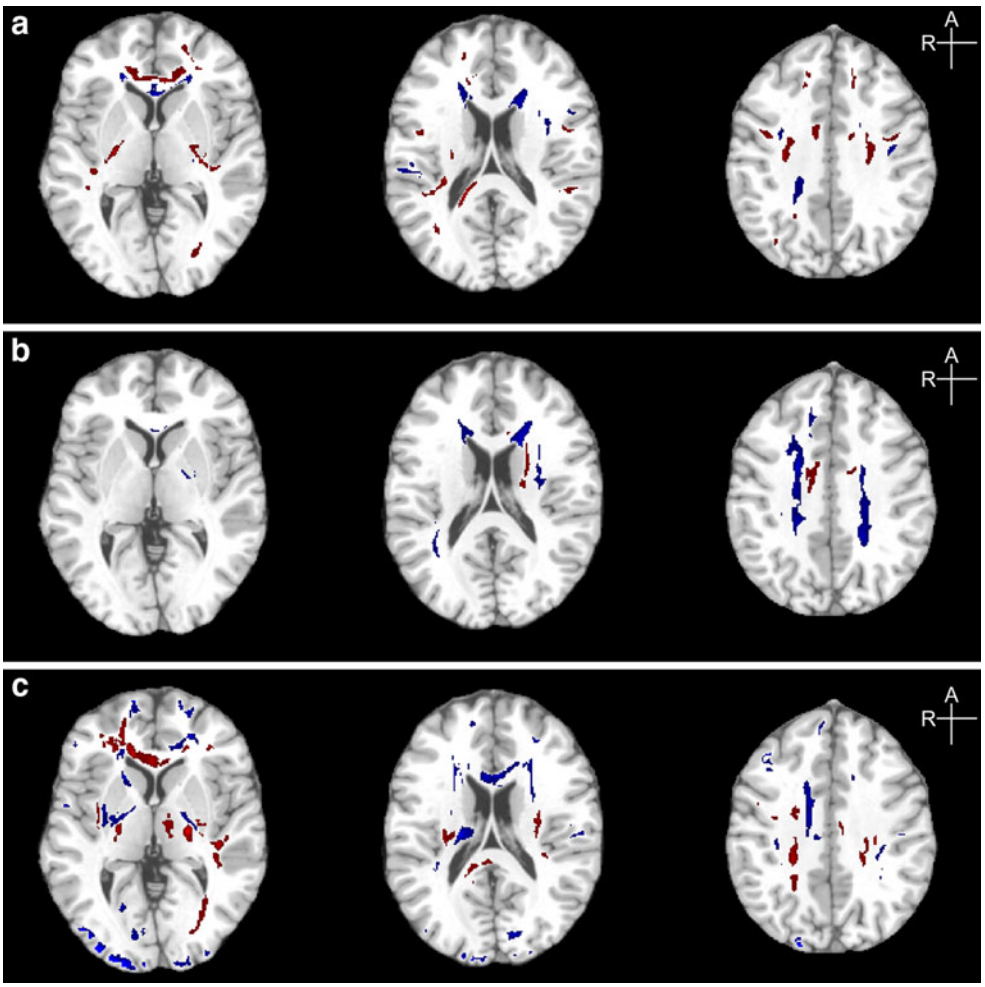

Fig. 1 Three axial images in three patients (**a**, **b**, **c**) showing multiple areas of abnormally high (*blue*) and low (*red*) FA in the acute post-injury period (<2 weeks: A- 3 days, B- 6 days, C- 9 days). Each patient shows multiple locations of abnormality, with variable lesion location across individuals

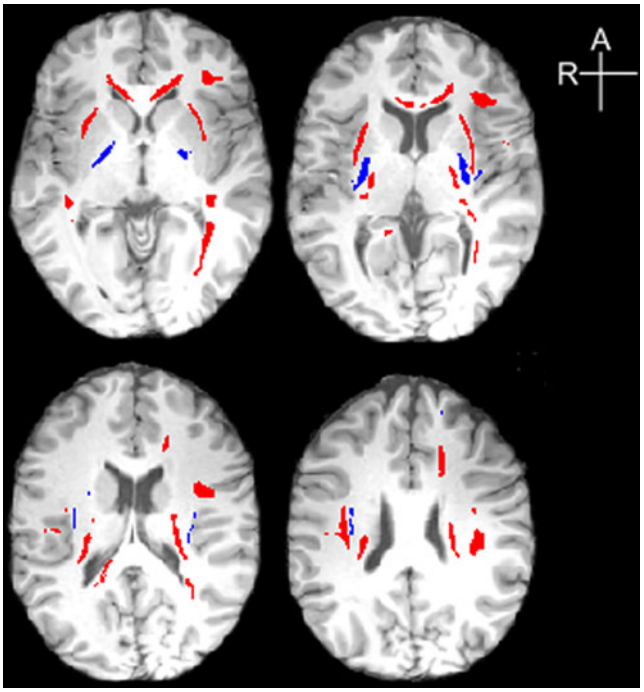

Fig. 2 Four axial images show regions of abnormal FA overlaid on the patient's own T1-weighted brain images

mTBI (Miles et al. 2008; Rutgers et al. 2008; Inglese et al. 2005) (see Shenton et al. 2012). FA has also been found to be robust for detection of axonal pathology in experimental studies (Bennett et al. 2012; Mac Donald et al. 2007c) (See Bigler and Maxwell 2012). Nonetheless, the EZ-MAP approach could be applied to maps of axial, radial or mean diffusivity, as well as other quantitative imaging parameters; this is an important area for future investigation.

Areas of abnormally low FA consistent with TAI were detected in almost all patients within 2 weeks of injury (32/34 patients). This finding is consistent with animal and human studies reporting the pathological substrates of diffusion anisotropy and imaging features of mTBI (e.g.,(Mac Donald et al. 2007c)). In white matter, water diffuses more readily parallel to axons because its diffusion in other directions is restricted by subcellular structure including neurofilaments, microtubules, myelin and the axolemma. Intra-axonal microstructural disturbances and degradation of the myelin sheath have been demonstrated using DTI, in the absence of frank axotomy (Song et al. 2003). The shear forces exerted on an axon during even mild head trauma have been reported to cause axonal pathology, with or without ultimate axotomy (Povlishock and Katz 2005) (see Bigler and Maxwell 2012). The study patients sustained mild head injury and as far as it is possible to know, they have no other reasons to have white matter disease. The cohort was carefully screened to exclude confounding variables and no patients had any visible abnormalities on conventional imaging. Our findings thus underscore the fact that mild head trauma causes actual brain injury and that it is detectable at the single subject level.

The abnormally high FA detected in the great majority (32/34 patients) of our patients within 2 weeks of injury is a particularly interesting finding. Biophysically, this phenomenon is unexpected because the loss or disruption of white matter microstructure by mTBI would be expected to manifest as low FA. However, in our study and several others, high FA in the corpus callosum has been detected 72 h (Bazarian et al. 2007), 6 days (45) and 2 weeks (Mayer et al. 2010) after mTBI. These few studies that have found and discussed findings of high FA have assessed patients close to the time of injury and generally put forth the explanation that axonal swelling in the acute post-injury period, due to an intracellular influx of water (i.e., cytotoxic edema), leads to restriction of diffusion within the extracellular space, resulting in increased anisotropic diffusion and therefore higher FA. However, a study of chronic mTBI patients also showed high FA in the internal capsule (Lo et al. 2009). A recent and elegant DTI and histological study of TBI in a rodent model demonstrated increase in anisotropy, which correlated with reactive astrogliosis (Budde et al. 2011). While this association raises additional possibilities for the mechanisms that may lead to increases in anisotropy and warrants further exploration, we note that the finding was limited to grey matter, as seen with both histology and DTI. White matter anisotropy was found to decline in association with markers of axonal injury and was not associated with astrogliosis. It thus remains unclear how gliosis might impact white matter anisotropy. Additionally, the injury model (controlled cortical impact) produced gross tissue disruption and at least a moderate degree of injury, features not present in human mTBI.

The time course of evolving high FA in the present study, though heterogeneous, provides some intriguing clues to pathophysiology. The finding of high FA in all patients at 3 and 6 months post-injury, as well as in chronic symptomatic mTBI patients (see below), is inconsistent with cytotoxic edema. Though present at 2 weeks, the number of voxels with high FA increased from 2 weeks to 3 months in most patients (11 of 16) and then declined from 3 months to 6 months in many (5 of 7). This profile suggests that elevated FA might represent a biophysical manifestation of a response to brain injury, rather than a direct manifestation of injury pathology.

Increased FA may reflect neuroplastic responses to injury, perhaps through up-regulation of active axoplasmic transport. Notably, local increases in anisotropy have been reported in training experiments, where the brain substrate is presumed to be plasticity (Scholz et al. 2009). Compensatory mechanisms may be most active during the acute and sub-acute periods when the opportunity for repair and recovery is maximal. Our observation of decreasing number of low FA voxels is consistent with repair of TAI, while the early increase in or

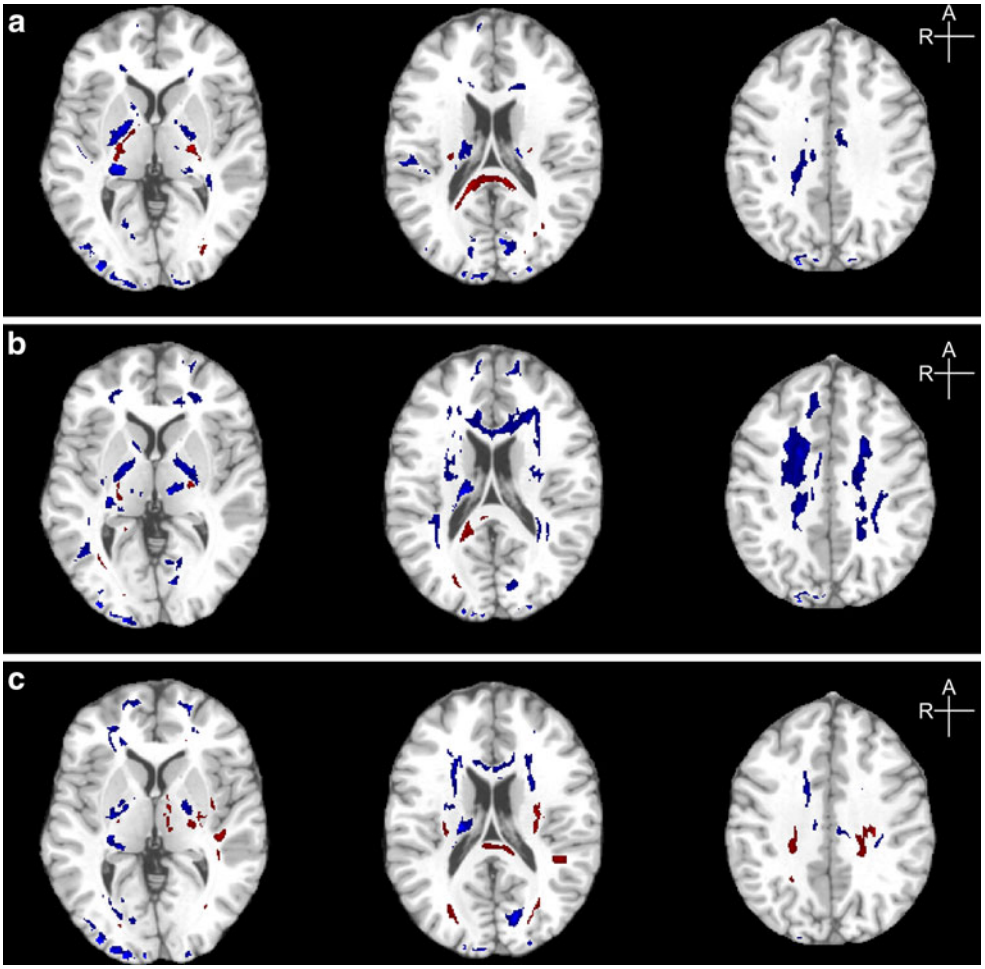

Fig. 3 Axial images at 3 month follow-up in the same three patients (**a**, **b**, **c**) shown in Fig. 1, again show multiple areas of abnormally high (*blue*) and low (*red*) FA. Each individual has unique pattern and number voxels expressing abnormal FA

Table 5 Change in the number of abnormal voxels between acute post-injury period (<2 weeks) and 3 months

Patient	Low FA		High FA	
	<2 weeks	3 months	<2 weeks	3 months
1	15139	5045	7345	24367
4	23420	14293	0	18995
5	5389	5528	14542	46653
8	621	442	1906	24686
10	1295	12765	4040	35543
12	2161	1095	1286	2132
14	1409	0	0	0
15	11766	13788	597	18175
18	9184	0	5624	1243
19	17673	10206	25760	20325
20	11827	10909	17392	18693
21	12524	20470	20282	22871
22	15927	1290	5013	1689
28	0	532	2928	4773
30	649	578	993	6126
31	14826	2924	13534	7856

maintenance of number of high FA voxels at 3 months, followed by a decrease in the number of high FA voxels at 6 months post-injury is consistent with the early development of plasticity and other compensatory mechanisms. Further study, including the differential contribution of specific Eigenvalues to abnormally elevated anisotropy may help to clarify the biological role of abnormally high FA.

The finding of high FA in nearly every patient begs the question as to why high FA has not been detected in most prior DTI studies of mTBI. Prior studies employed group-wise analyses, which are inherently insensitive to variability in the spatial location of abnormalities between patients. We have shown much variability in the spatial distribution of high FA voxels between patients, which would likely be missed by a group-wise approach.

Outside of the specific study recruitment, we have had the opportunity to examine many chronic (more than 1 year post-mTBI) symptomatic mTBI patients referred for clinical imaging and can report that they too show areas of abnormally high and low FA. Three patients randomly selected from this clinical patient group are shown as examples in Fig. 7. While brain loci characteristic of TBI (e.g., corpus callosum) were detected as abnormal in these patients, the

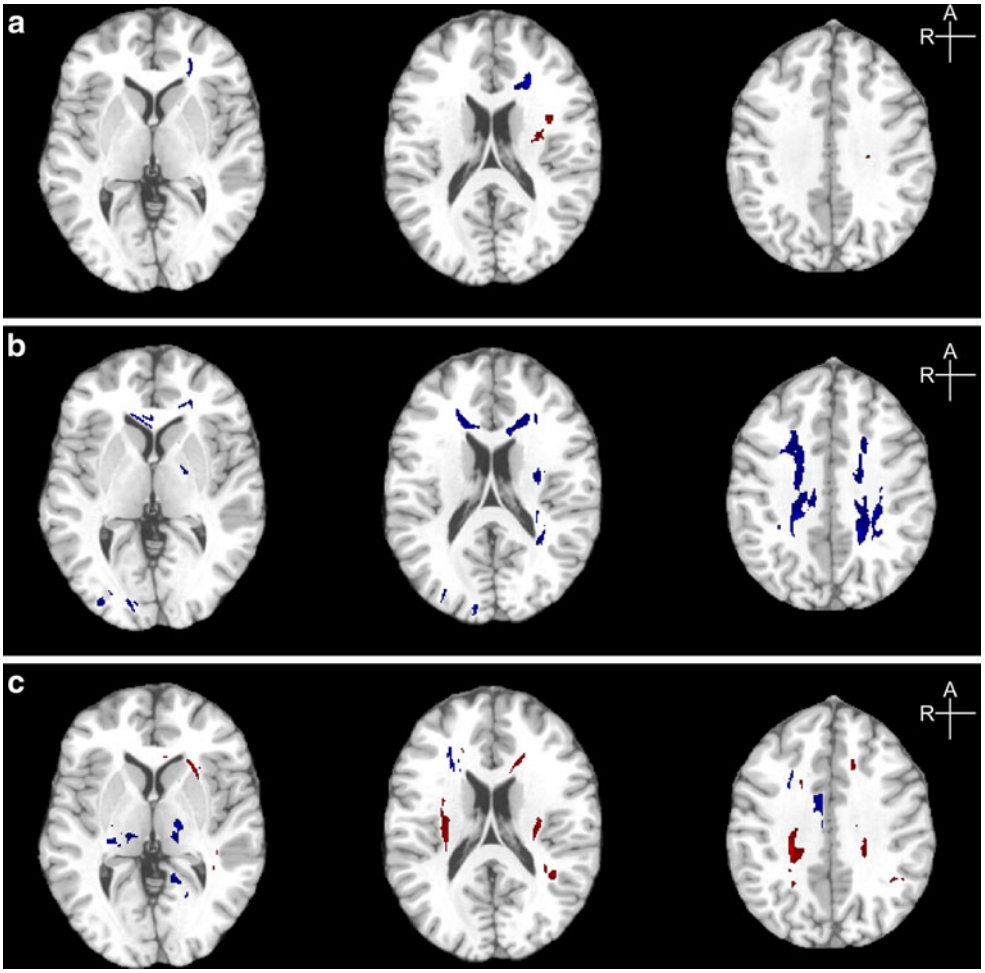

Fig. 4 Axial images at 6 month follow-up in the same three patients (**a**, **b**, **c**) shown in Figs. 1 and 3, again show multiple areas of abnormally high (*blue*) and low (*red*) FA, with a unique pattern and number voxels expressing abnormal FA in each individual

Table 6 Change over time in the number of abnormal voxels (<2 weeks, 3 months, and 6 months)

	Low FA			High FA		
	<2 weeks	3 months	6 month	<2 weeks	3 months	6 months
1	15139	5045	1176	7345	24367	1820
5	5389	5528	1411	14542	46653	20683
10	1295	12765	0	4040	35543	979
12	2161	1095	2179	1286	2132	4944
14	1409	0	0	0	0	694
19	17673	10206	12153	25760	20325	3488
21	12524	20470	17426	20282	22871	3130
6	2352	NA	0	11078	NA	1746
7	38943	NA	6681	19750	NA	4409
11	1246	NA	3792	1574	NA	2986
Mean	7941	7873	4906	10465	21699	5105
SD	7003	7182	6964	9931	16725	7030

NA – Not available, because the patient failed to come in for the follow up visit

Mean and SD were calculated for each time period with the number of abnormal voxels from 7 patients who completed all 3 follow-ups

locations of abnormality were widespread and varied between patients.

Several limitations of this study must be considered. Voxelwise analysis approaches, particularly in individual subjects, may be prone to false positive results. This is because many simultaneous statistical tests are performed. Vulnerability to false positive inference is perhaps the central limitation of such approaches. We therefore take many steps to minimize the chance of such type 1 errors. Two levels of thresholding are employed, such that initially any voxel must meet a threshold (α_1) to *potentially* be identified as an abnormality. Next, contiguous subsets of these voxels are identified as abnormalities only if the size of the cluster of such voxels meets a second threshold (α_2). This second threshold is determined based on GRF and is corrected for multiple comparisons. The rationale for the dual threshold approach is that while multiple testing increases the chance for type 1 error at the individual voxel level, these chance errors should be randomly distributed throughout the brain volume. It is not statistically plausible that such random errors will cluster in a contiguous region of the size we require for a final determination of abnormality. It is important to note that the results reported here are based on thresholds (α_1, α_2) shown to maximize discrimination of

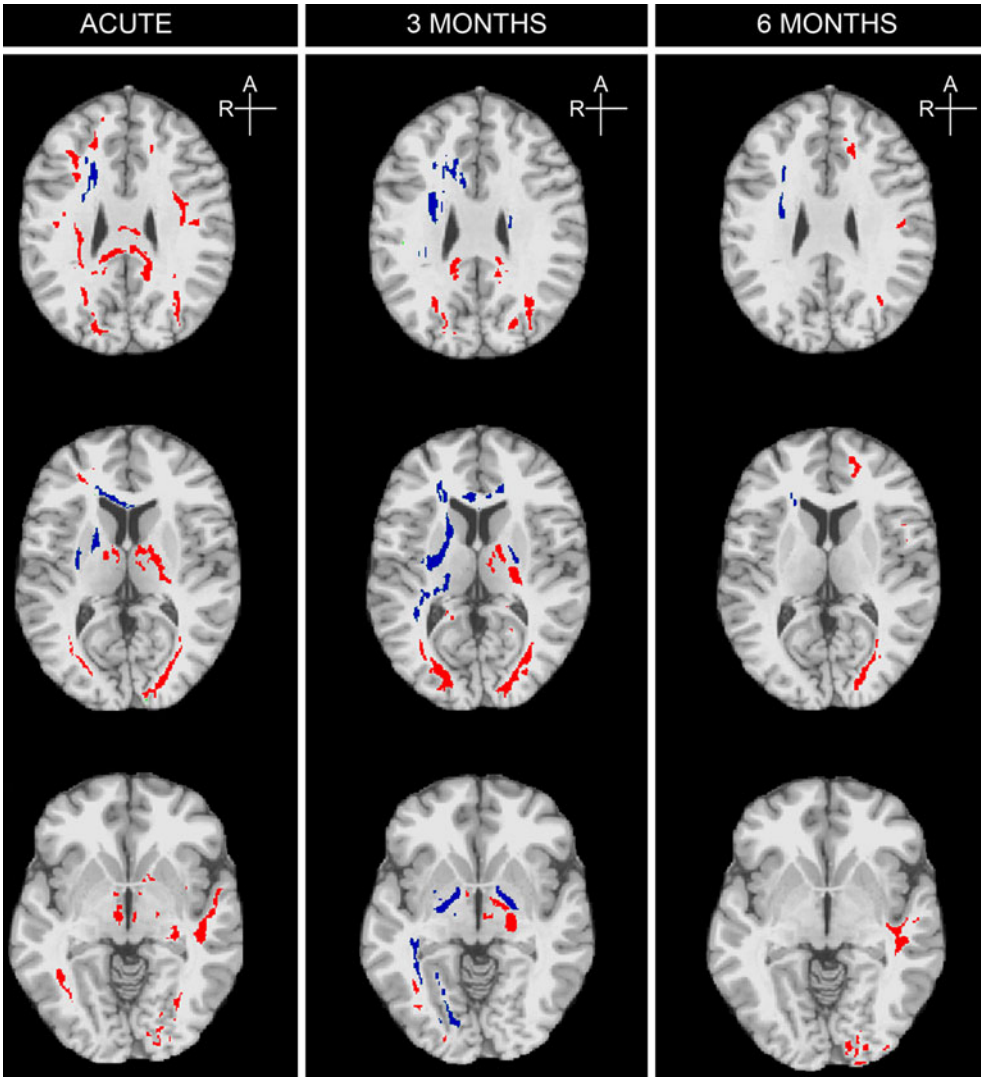

Fig. 5 Abnormal FA detected by 1-sample T-test. Each column shows abnormal regions detected within 2 weeks of injury, at 3 months and at 6 months, respectively, showing an increasing number of abnormally high FA voxels (*blue*) at 3 months followed by a decrease at 6 months. The number of abnormally low FA voxels (*red*) decreases at 3 and 6 months in comparison to the initial assessment. These findings are consistent with the patterns found in individual patients (Figs. 1, 3, 4)

patients and controls. At these thresholds, the chance of finding a single suprathreshold cluster is less than 1 %. However, it is important to recognize that sensitivity and specificity vary based on the selected thresholds. Depending on the clinical or

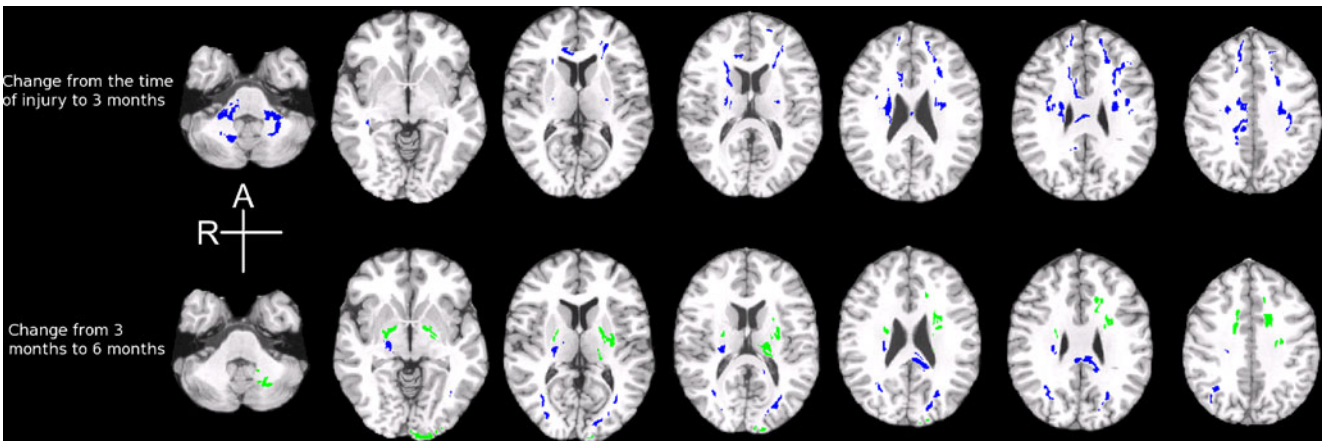

Fig. 6 Change in FA detected by voxelwise paired T-test. The top row shows change from the time of injury to 3 months and the bottom row from 3 to 6 months. Significant change is shown in each example slice. Blue indicates increase in FA and green indicates decrease in FA over the follow-up interval

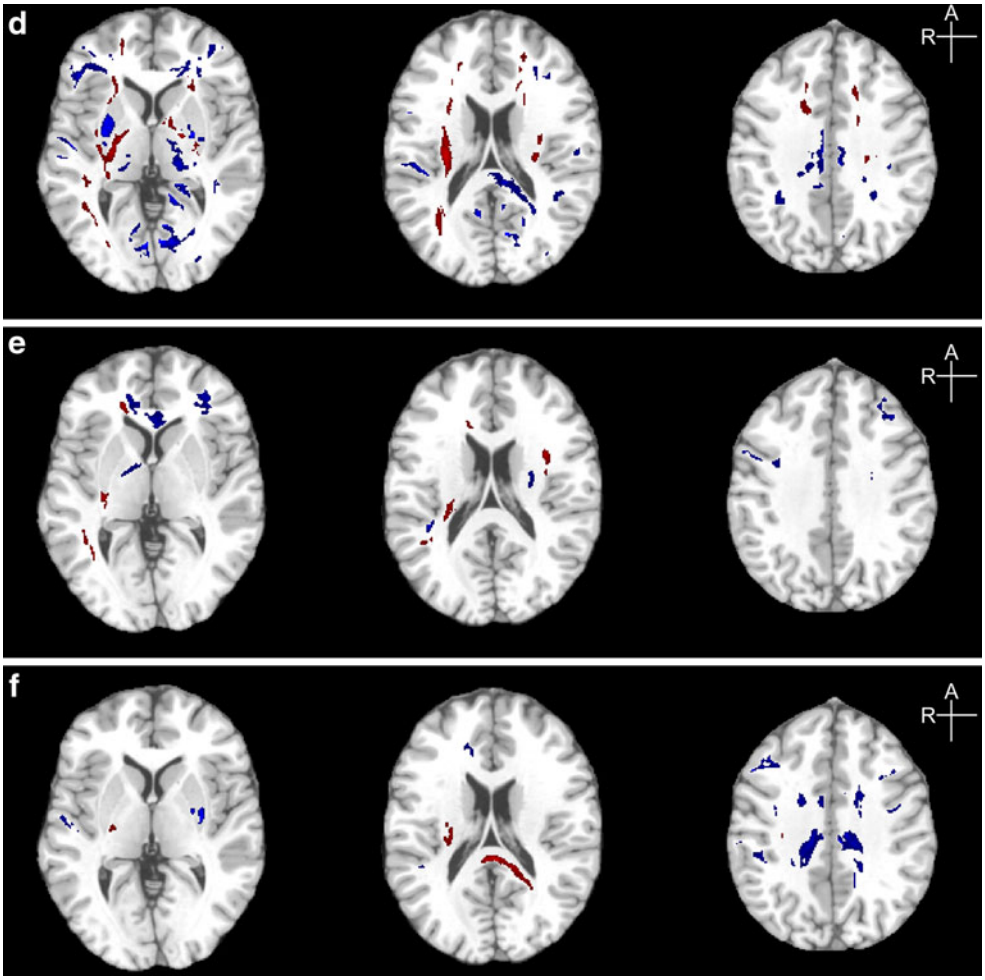

Fig. 7 Areas of abnormal FA in three chronic mTBI patients (**d**, **e**, **f**). As in the study population, these patients also demonstrate focal areas of both high and low FA

research question, a different threshold level might be more appropriate. Specifically, the use of a stricter threshold reduces the chance of a false positive inference (i.e., misclassifying a normal subject as a patient), though at the expense of sensitivity.

A voxelwise analysis provides powerful means for surveying the entire brain for abnormalities and the only means for appreciating the scope of inter-individual differences in the spatial distribution of pathology. An additional advantage of the approach is that it is not subject to the observer bias inherent in the manual delineation of ROIs or tractograms. Nonetheless, the spatial normalization prerequisite to a voxelwise analysis is a potential source of error. This is especially so if distortion is present in the original diffusion-weighted images due to eddy current or magnetic susceptibility-related effects. Images were corrected for the effects of eddy currents and we employed a validated method to correct for distortion prior to image analysis. To ensure that registration of different image types (DTI and MP-RAGE) as well as registration of images from individual subjects would be as accurate as possible, each subject's eddy current and motion corrected DTI images was registered to their own T2-weighted FSE images, which were subsequently registered to their own high-resolution T1-weighted images and, finally, to a high-resolution T1-weighted template (the MNI atlas brain). We specifically employ a locally implemented template that has been extensively tested to ensure excellent registration of subject data. This approach minimizes the potential for error in inter-modality inter-subject registration. The registration approach employed has been compared to several other methods including AIR, AFNI and SPM (Ardekani 1995; Ardekani et al. 2005) and performs equal to or better than all. Another issue inherent in the spatial normalization process is that the native resolution of the DTI images is coarse relative to the higher resolution structural images. During spatial normalization, DTI voxels are resampled to this higher resolution. It is important to recognize that the native voxel thus interpolated to multiple smaller voxels does not support inference regarding this finer spatial scale. Ultimately, what we can learn from the data remains limited to effects detectable on the scale of the native DTI resolution.

It is well known that FA is reduced at locations where white matter fibers cross within a voxel [e.g., (Poupon et al. 2000)]. Such regions of low FA due to fiber crossing could possibly be detected as pathologically abnormal FA. However, since crossing fibers tend to occur in the same location across subjects, a systematic difference in crossing fiber anatomy

between a patient and the control group is not likely and therefore not likely to be detected as abnormal, although where a single patient is compared to a group of normals, the risk for this problem may be somewhat greater than in a group vs. group comparison.

As is a common problem in longitudinal studies, particularly in patients with variable actual and perceived impairment, we encountered significant attrition during follow-up. This limits our sample size at the three and six month follow-up assessments. Additionally, while we do not have specific reason to suspect bias, is possible that attrition during follow-up could lead to selection bias, were patients either more or less severely injured or impaired selectively more or less likely to comply with follow-up.

Controls and patients reported different educational experience, which was significant. Although it would be ideal to control for this variable during subject recruitment, as we did with age and gender, this difference has been accounted for using standard approaches. In addition, the effect of education on FA was tested and found to be quite modest (Kim et al. 2011).

In conclusion, EZ-MAP detects multifocal abnormally low and high FA, consistent with TAI and, we propose, plasticity or other compensatory processes, respectively. This effective individual level assessment of mTBI yields patient-specific information. Such individual measurements can be used to assess the relationship of each patient's injury to their functional outcome, which is an essential step toward determining the utility of DTI as a prognostic biomarker, which might serve to guide future personalized medicine approaches to the treatment of mTBI.

Appendix: Data analysis procedures

Adjustment for demographic covariate effects

We chose control subjects with an even distribution of age, gender and educational attainment that fully brackets the range of the patients; no patient age or educational attainment exceeds all controls at either extreme. FA images used in subsequent analyses were adjusted by regression coefficients (age, gender, years of education) estimated from control subjects at each voxel. Regression coefficients thus determined were applied to FA images of the patients, but only at locations where effects on individual voxels were significant at $p<0.05$ and where more than 100 significant voxels formed a contiguous cluster.

Enhanced Z-score (EZ)

We computed the Z-score defined by $Z=(X-mean)/SD$ at each voxel (i) within a patient's FA volume with reference values (mean and Standard Deviation (SD)) computed from the control group. It therefore follows that Z-score of a patient may vary with the composition of the control group, with potential for unreliable inferences when the reference group is small. We employed a bootstrap procedure to overcome this potential for sample-to-sample variation of Z-scores, and calculated EZ-score by $EZ=Z/\widehat{\sigma}$, where $\widehat{\sigma}$ is the bootstrap SD estimate of Z-scores at a voxel. We applied two levels of thresholding to identify significantly abnormal voxels. First, each voxel must meet a threshold, |EZ|>1.96. Second, the subset of these voxels that forms contiguous clusters meeting a size threshold (1 %) based on the Gaussian Random Field (GRF) theory (Friston et al. 1994); the cluster size threshold is corrected for multiple comparisons. These thresholds provide maximal discrimination of patients and controls based on maximal area under the ROC curve (results presented previously (Kim et al. 2011)) determined from a range of thresholds (voxel z-score: 2.5758 and 1.96; cluster size: 0.01 (corrected), 0.05 (corrected), 0.01 (uncorrected) and 0.05 (uncorrected)). It is important to recognize that some voxels meeting the criteria for abnormality are found in controls when these optimal thresholds are applied. We therefore tested the difference in the numbers of abnormal voxels between patients (n=34) and unique normal control subjects (n=21) (i.e., not the same individuals used to compute the reference mean and SD for use in the E-Z calculation). The mean number of abnormal voxels found in patients was significantly greater than that of controls (p=0.014, 2-tails) (Kim et al. 2011).

One Sample t-Test:

An Enhanced Z-score (EZ_i) of i^{th} mTBI patient at a voxel (voxel location index is omitted) is written as $EZ_i=\frac{X_i-\overline{Y}}{S_Y\widehat{\sigma^B}}$, where X_i is FA of i^{th} patient; $(\overline{Y}, S_Y)$ is mean and SD of control group, respectively; $\widehat{\sigma}^B$ is bootstrap SD estimate of Z-scores. T-score for the 1-sample t-Test with null hypothesis that is the mean Enhanced Z-scores of patients would be equal to zero is written as

$$T=\frac{\sqrt{n_x}E\overline{Z}}{SD(EZ)}=\frac{\sqrt{n_x}(\overline{X}-\overline{Y})}{SD(EZ)S_Y\widehat{\sigma}^B}=\frac{\sqrt{n_x}(\overline{X}-\overline{Y})}{S_X}\sim t(n_x-1). \quad (1)$$

since $SD(EZ_i)=\frac{S_X}{S_Y\widehat{\sigma^B}}$ (SD of Enhanced Z-scores of patients), where S_x is SD of FAs from patients, and n_x is the number of patient.

References

Ardekani, B. (1995). A fully automatic multimodality image registration algorithm. *Journal of Computer Assisted Tomography, 19*(4), 615–623.

Ardekani, B., Guckemus, S., Bachman, A., Hoptman, M. J., Wojtaszek, M., & Nierenberg, J. (2005). Quantitative comparison of algorithms for inter-subject registration of 3D volumetric brain MRI scans. *Journal of Neuroscience Methods, 142*(1), 67–76.

Bazarian, J. J., Zhong, J., Blyth, B., Zhu, T., Kavcic, V., & Peterson, D. (2007). Diffusion tensor imaging detects clinically important axonal damage after mild traumatic brain injury: a pilot study. [Article]. *Journal of Neurotrauma, 24*(9), 1447–1459. doi:10.1089/neu.2007.0241.

Bennett, R. E., Mac Donald, C. L., & Brody, D. L. (2012). Diffusion tensor imaging detects axonal injury in a mouse model of repetitive closed-skull traumatic brain injury. *Neuroscience Letters*. doi:10.1016/j.neulet.2012.02.024.

Bigler, E. D. & Maxwell, W. L. (2012). Neuropathology of mild traumatic brain injury: relationship to neuroimaging findings. *Brain Imaging and Behavior*. This special issue.

Budde, M. D., Janes, L., Gold, E., Turtzo, L. C., & Frank, J. A. (2011). The contribution of gliosis to diffusion tensor anisotropy and tractography following traumatic brain injury: validation in the rat using Fourier analysis of stained tissue sections. [Research Support, N.I.H., Intramural Research Support, Non-U.S. Gov't]. *Brain: A journal of neurology, 134*(Pt 8), 2248–2260. doi:10.1093/brain/awr161.

Crooks, D. (1991). The pathological concept of diffuse axonal injury: its pathogenesis and the assessment of severity. *The Journal of Pathology, 165*(1), 5–10.

Esselman, P., & Uomoto, J. M. (1995). Classification of the spectrum of mild traumatic brain injury. *Brain Injury, 9*(4), 417–424.

Friston, K. J., Worsley, K. J., Frackowiak, R. S. J., Mazziotta, J. C., & Evans, A. C. (1994). Assessing the significance of focal activations using their spatial extent. *Human Brain Mapping, 1*, 210–220.

Geary, E. K., Kraus, M. F., Pliskin, N. H., & Little, D. M. (2010). Verbal learning differences in chronic mild traumatic brain injury. *Journal of the International Neuropsychological Society, 16*(3), 506–516. doi:10.1017/S135561771000010X.

Greer, J. E., McGinn, M. J., & Povlishock, J. T. (2011). Diffuse traumatic axonal injury in the mouse induces atrophy, c-Jun activation, and axonal outgrowth in the axotomized neuronal population. *Journal of Neuroscience, 31*(13), 5089–5105. doi:10.1523/jneurosci.5103-10.2011.

Hammoud, D., & Wasserman, B. A. (2002). Diffuse axonal injuries: a pathophysiology and imaging. *Neuroimaging Clinics of North America, 12*(2), 205–216.

Hartikainen, K. M., Waljas, M., Isoviita, T., Dastidar, P., Liimatainen, S., Solbakk, A. K., et al. (2010). Persistent symptoms in mild to moderate traumatic brain injury associated with executive dysfunction. *Journal of Clinical and Experimental Neuropsychology, 1–8*. doi:10.1080/13803390903521000.

Holmes, C., Hoge, R., Collins, L., Woods, R., Toga, A. W., & Evans, A. C. (1998). Enhancement of MR images using registration for signal averaging. *Journal of Computer Assisted Tomography, 22*(2), 324–333.

Inglese, M., Makani, S., Johnson, G., Cohen, B. A., Silver, J. A., Gonen, O., et al. (2005). Diffuse axonal injury in mild traumatic brain injury: a diffusion tensor imaging study. *Journal of Neurosurgery, 103*(2), 298–303.

Kim, N., Hulkower, M. B., Park, Y., Gardin, T. M., Smith, J. L., Branch, C. A., et al. (2011). *Robust Detection of White Matter Injury in Individual Patients After Mild Traumatic Brain Injury* Paper presented at the ISMRM 19th Annual Meeting and Exhibition, Montreal, Canada, May 9, 2011.

Kou, Z., Wu, Z., Tong, K. A., Holshouser, B., Benson, R. R., Hu, J., et al. (2010). The role of advanced MR imaging findings as biomarkers of traumatic brain injury. *The Journal of Head Trauma Rehabilitation, 25*(4), 267–282. doi:10.1097/HTR.0b013e3181e54793.

Kraus, M. F., Susmaras, T., Caughlin, B. P., Walker, C. J., Sweeney, J. A., & Little, D. M. (2007). White matter integrity and cognition in chronic traumatic brain injury: a diffusion tensor imaging study. [Article]. *Brain, 130*, 2508–2519. doi:10.1093/brain/awm216.

Levin, H. S., Wilde, E., Troyanskaya, M., Petersen, N. J., Scheibel, R., Newsome, M., et al. (2010). Diffusion tensor imaging of mild to moderate blast-related traumatic brain injury and its sequelae. *Journal of Neurotrauma, 27*(4), 683–694. doi:doi:10.1089/neu.2009.1073.

Lim, K., Ardekani, B. A., Nierenberg, J., Butler, P. D., Javitt, D. C., & Hoptman, M. J. (2006). Voxelwise correlational analyses of white matter integrity in multiple cognitive domains in schizophrenia. *The American Journal of Psychiatry, 163*(11), 2008–2010.

Lipton, M. L., Gulko, E., Zimmerman, M. E., Friedman, B. W., Kim, M., Gelella, E., et al. (2009). Diffusion tensor imaging implicates prefrontal axonal injury in executive function impairment following mild traumatic brain injury. *Radiology, 252*(3), 816–824.

Little, D. M., Kraus, M. F., Joseph, J., Geary, E. K., Susmaras, T., Zhou, X. J., et al. (2010). Thalamic integrity underlies executive dysfunction in traumatic brain injury. *Neurology, 74*(7), 558–564. doi:10.1212/WNL.0b013e3181cff5d5.

Lo, C., Shifteh, K., Gold, T., Bello, J. A., & Lipton, M. L. (2009). Diffusion tensor imaging abnormalities in patients with mild traumatic brain injury and neurocognitive impairment. *Journal of Computer Assisted Tomography, 33*(2), 293–297.

Mac Donald, C., Dikranian, K., Bayly, P., Holtzman, D., & Brody, D. (2007a). Diffusion tensor imaging reliably detects experimental traumatic axonal injury and indicates approximate time of injury. *Journal of Neuroscience, 27*(44), 11869–11876.

Mac Donald, C., Dikranian, K., Song, S. K., Bayly, P. V., Holtzman, D. M., & Brody, D. L. (2007b). Detection of traumatic axonal injury with diffusion tensor imaging in a mouse model of traumatic brain injury. *Experimental Neurology, 205*(1), 116–131.

Mac Donald, C. L., Dikranian, K., Bayly, P., Holtzman, D., & Brody, D. (2007c). Diffusion tensor imaging reliably detects experimental traumatic axonal injury and indicates approximate time of injury. *Journal of Neuroscience, 27*(44), 11869–11876. doi:10.1523/jneurosci.3647-07.2007.

Mayer, A. R., Ling, J., Mannell, M. V., Gasparovic, C., Phillips, J. P., Doezema, D., et al. (2010). A prospective diffusion tensor imaging study in mild traumatic brain injury. *Neurology, 74*(8), 643–650. doi:10.1212/WNL.0b013e3181d0ccdd.

McArthur, D., Chute, D. J., & Villablanca, J. P. (2004). Moderate and severe traumatic brain injury: epidemiologic, imaging and neuropathologic perspectives. *Brain Pathology, 14*(2), 185–194.

Meythaler, J. M., Peduzzi, J. D., Eleftheriou, E., & Novack, T. A. (2001). Current concepts: diffuse axonal injury-associated traumatic brain injury. *Archives of Physical Medicine and Rehabilitation, 82*(10), 1461–1471.

Miles, L., Grossman, R. I., Johnson, G., Babb, J. S., Diller, L., & Inglese, M. (2008). Short-term DTI predictors of cognitive dysfunction in mild traumatic brain injury. *Brain Injury, 22*(2), 115–122.

Muller, H. P., Unrath, A., Riecker, A., Pinkhardt, E. H., Ludolph, A. C., & Kassubek, J. (2009). Intersubject variability in the analysis of diffusion tensor images at the group level: fractional anisotropy mapping and fiber tracking techniques. *Magnetic Resonance Imaging, 27*(3), 324–334. doi:10.1016/j.mri.2008.07.003.

Niogi, S. N., Mukherjee, P., Ghajar, J., Johnson, C., Kolster, R. A., Sarkar, R., et al. (2008a). Extent of microstructural white matter injury in postconcussive syndrome correlates with impaired cognitive reaction time: a 3T diffusion tensor imaging study of mild traumatic brain injury. *AJNR. American Journal of Neuroradiology, 29*(5), 967–973. doi:10.3174/ajnr.A0970.

Niogi, S. N., Mukherjee, P., Ghajar, J., Johnson, C. E., Kolster, R., Lee, H., et al. (2008b). Structural dissociation of attentional control and memory in adults with and without mild traumatic brain injury. *Brain, 131*(Pt 12), 3209–3221. doi:10.1093/brain/awn247.

Oishi, K., Faria, A. V., & Mori, S. (2010). JHU-MNI-ss Atlas.

Pettus, E., Christman, C. W., Giebel, M. L., & Povlishock, J. T. (1994). Traumatically induced altered membrane permeability: its relationship to traumatically induced reactive axonal change. *Journal of Neurotrauma, 11*(5), 507–522.

Poupon, C., Clark, C. A., Frouin, V., Regis, J., Bloch, I., Le Bihan, D., et al. (2000). Regularization of diffusion-based direction maps for the tracking of brain white matter fascicles. *NeuroImage, 12*(2), 184–195. doi:10.1006/nimg.2000.0607.

Povlishock, J. (1986). Traumatically induced axonal damage without concomitant change in focally related neuronal somata and dendrites. *Acta Neuropathologica, 70*(1), 53–59.

Povlishock, J. (1992). Traumatically induced axonal injury: pathogenesis and pathobiological implications. *Brain Pathology, 2*(1), 1–12.

Povlishock, J., & Katz, D. I. (2005). Update of neuropathology and neurological recovery after traumatic brain injury. *The Journal of Head Trauma Rehabilitation, 20*(1), 76–94.

Povlishock, J. T., Becker, D. P., Cheng, C. L., & Vaughan, G. W. (1983). Axonal change in minor head injury. *Journal of Neuropathology and Experimental Neurology, 42*(3), 225–242.

Rosenbaum, S. B. & Lipton, M. L. (2012). Embracing chaos: the scope and importance of clinical and pathological heterogeneity in mTBI. *Brain Imaging and Behavior*. This special issue.

Rubovitch, V., Ten-Bosch, M., Zohar, O., Harrison, C. R., Tempel-Brami, C., Stein, E., et al. (2011). A mouse model of blast-induced mild traumatic brain injury. *Experimental Neurology, 232*(2), 280–289. doi:10.1016/j.expneurol.2011.09.018.

Rutgers, D. R., Toulgoat, F., Cazejust, J., Fillard, P., Lasjaunias, P., & Ducreux, D. (2008). White matter abnormalities in mild traumatic brain injury: a diffusion tensor imaging study. [Proceedings Paper]. *American Journal of Neuroradiology, 29*(3), 514–519. doi:10.3174/ajnr.A0856.

Scholz, J., Klein, M. C., Behrens, T. E., & Johansen-Berg, H. (2009). Training induces changes in white-matter architecture. [Research Support, Non-U.S. Gov't]. *Nature Neuroscience, 12*(11), 1370–1371. 10.1038/nn.2412.

Sharp, D. J., & Ham, T. E. (2011). Investigating white matter injury after mild traumatic brain injury. *Current Opinion in Neurology, 24*(6), 558–563. doi:10.1097/WCO.0b013e32834cd523.

Shenton, M. E., Hamoda, H. M., Schneiderman, J. S., Bouix, S., Pasternak, O., Rathi, Y., et al. (2012). A review of magnetic resonance imaging and diffusion tensor imaging findings in mild traumatic brain injury. *Brain Imaging and Behavior*. This special issue.

Smith, S., Jenkinson, M., Woolrich, M. W., et al. (2004). Advances in functional and structural MR image analysis and implementation as FSL. *NeuroImage, 23*(suppl 1), S208–S219.

Smith, S., Johansen-Berg, H., Jenkinson, M., et al. (2007). Acquisition and voxelwise analysis of multi-subject diffusion data with tract-based spatial statistics. *Nature Protocols, 2*(3), 499–503.

Song, S., Sun, S. W., Ju, W. K., Lin, S. J., Cross, A. H., & Neufeld, A. H. (2003). Diffusion tensor imaging detects and differentiates axon and myelin degeneration in mouse optic nerve after retinal ischemia. *NeuroImage, 20*(3), 1714–1722.

Spain, A., Daumas, S., Lifshitz, J., Rhodes, J., Andrews, P. J., Horsburgh, K., et al. (2010). Mild fluid percussion injury in mice produces evolving selective axonal pathology and cognitive deficits relevant to human brain injury. *Journal of Neurotrauma, 27*(8), 1429–1438. doi:10.1089/neu.2010.1288.

Wang, S., Wu, E. X., Qiu, D., Leung, L. H., Lau, H. F., & Khong, P. L. (2009). Longitudinal diffusion tensor magnetic resonance imaging study of radiation-induced white matter damage in a rat model. *Cancer Research, 69*(3), 1190–1198.